NeuroImage 159 (2017) 473–487

Contents lists available at ScienceDirect

NeuroImage

journal homepage: www.elsevier.com/locate/neuroimage

# Anatomical and functional properties of the foot and leg representation in areas 3b, 1 and 2 of primary somatosensory cortex in humans: A 7T fMRI study

Michel Akselrod [a,b,f,h,*], Roberto Martuzzi [a,b,c], Andrea Serino [a,b,h], Wietske van der Zwaag [d,e], Roger Gassert [f], Olaf Blanke [a,b,g,*]

[a] Center for Neuroprosthetics, Swiss Federal Institute of Technology of Lausanne (EPFL), Lausanne, Switzerland
[b] Laboratory of Cognitive Neuroscience, Swiss Federal Institute of Technology of Lausanne (EPFL), Lausanne, Switzerland
[c] Foundation Campus Biotech Geneva, Geneva, Switzerland
[d] Biomedical Imaging Research Center, Swiss Federal Institute of Technology of Lausanne (EPFL), Lausanne, Switzerland
[e] Spinoza Centre for Neuroimaging, Amsterdam, The Netherlands
[f] Rehabilitation Engineering Laboratory, Swiss Federal Institute of Technology of Zurich, Zurich, Switzerland
[g] Department of Neurology, University Hospital, Geneva, Switzerland
[h] Laboratory MySpace, University Hospital of Lausanne (CHUV), Lausanne, Switzerland

ARTICLE INFO

*Keywords:*
Primary somatosensory cortex
Brodmann areas 3b-1-2
Lower limb representation
Somatotopy
7 T fMRI

ABSTRACT

Primary somatosensory cortex (S1) processes somatosensory information and is composed of multiple subregions. In particular, tactile information from the skin is encoded in three subregions, namely Brodmann areas (BAs) 3b, 1 and 2, with each area representing a complete map of the contralateral body. Although, much is known about the somatotopic organization of the hand in human S1, less research has been carried out regarding the somatotopic maps of the foot and leg in S1. Moreover, a latero-medial S1 organization along the superior part of the post-central gyrus has been reported when moving from hip to toes, yet to date there is no study investigating leg/foot maps within the different subregions of S1. Using ultra-high field MRI (7 T), we mapped six cortical representations of the lower limb (hip to toes) at the single subject level and performed this analysis separately for BAs 3b, 1 and 2. Analyzing the BOLD responses associated with tactile stimulations of the mapped foot and leg regions on each side, we quantified the extent and the strength of activation to determine somatotopic organization. In addition, we investigated whether each mapped representation also responded to the stimulation of other body parts (i.e. response selectivity) and conducted dissimilarity analysis relating these anatomical and functional properties of S1 to the physical structure of the lower limbs. Our data reveal somatotopy for the leg, but not for the foot in all investigated BAs, with large inter-subject variability. We found only minor differences between the properties of the three investigated BAs, suggesting that S1 maps for the lower limbs differ from those described for the hand. We also describe greater extent/strength of S1 activation for the big toe representation (compared to the other mapped representations) within all BAs, suggesting a possible homology between the first digit of upper and lower extremity in humans, and report different patterns of selectivity in the foot representations (i.e. lower selectivity) compared to the other leg representations (i.e. greater selectivity). These data provide a detailed description of human S1 subregions for the foot and leg, highlight the importance of high-resolution mapping studies and of single subject analysis, and indicate potential differences between the lower and the upper limb.

## Introduction

Magnetic Resonance Imaging (MRI) is one of the major non-invasive neuroimaging modalities. Compared to the widely established 3 T MRI, the increased signal-to-noise ratio of ultra-high field MRI (7 T) improves the spatial resolution to the millimeter or even sub-millimeter scale (van der Zwaag et al., 2009). Ultra-high field fMRI has already been applied to the study of the retinotopic organization of the human primary visual

* Correspondence to: Laboratory of Cognitive Neuroscience, Center for Neuroprosthetics, Ecole Polytechnique Fédérale de Lausanne, Campus Biotech H4, Chemin des Mines 9, CH-1202 Geneva, Switzerland.
*E-mail addresses:* michel.akselrod@gmail.com (M. Akselrod), olaf.blanke@epfl.ch (O. Blanke).

https://doi.org/10.1016/j.neuroimage.2017.06.021
Received 1 February 2017; Accepted 9 June 2017
Available online 17 June 2017

cortex (Olman et al., 2010), the tonotopic organization of the human primary auditory cortex (Da Costa et al., 2011), as well as the somatotopic organization in primary somatosensory cortex (S1) (Besle et al., 2014; Martuzzi et al., 2014). Considering the large inter-subject variability of S1 somatotopy, it has been proposed that, in particular, S1 responses should be studied at the single subject level (Pfannmöller et al., 2016), which can be achieved with high resolution at 7 T. However, previous somatotopic descriptions of human S1 were so far limited to the representations of single fingers with only few neuroimaging studies targeting important S1 representations of body parts other than the hand, such as the foot and the leg (Bao et al., 2012; Nakagoshi et al., 2005; Saadon-Grosman et al., 2015).

S1 is somatotopically organized to form a cortical map of the body, meaning that there is a point-to-point correspondence between the skin and S1 representations (Penfield and Boldrey, 1937; Rasmussen and Penfield, 1947). Primate S1 is located in the postcentral gyrus and contains three different cytoarchitectonic regions involved in the processing of tactile information, namely Brodmann Areas (BAs) 3b, 1, and 2 (Jones et al., 1978). BA 3b is located on the anterior wall of the postcentral gyrus, BA 1 on the crown, and BA 2 on the posterior wall (Geyer et al., 1999, 2000; Grefkes et al., 2001). Studies conducted in non-human primates showed that each of these BAs is somatotopically organized, with each body part being represented at a precise cortical position (Kaas et al., 1979; Merzenich et al., 1978; Nelson et al., 1980). Concerning tactile processing in S1, research in non-human primates showed that moving from BA 3b to BA 1 and BA 2, neurons progressively have larger receptive fields, responding to tactile information coming from larger portions of the skin, and also encode more complex tactile features, such as stimulus orientation and direction (Costanzo and Gardner, 1980; Gardner, 1988), suggesting that tactile information is hierarchically processed in the different BAs (Iwamura, 1998). Consistently with what has been observed in non-human primates, recent work using 7 T fMRI has shown that response selectivity is increased in human BA 3b compared to BA 1 and BA 2, i.e. that voxels in BA 3b respond to single finger stimulation (more selective) while voxels in BA 1 and BA 2 respond to the stimulation of multiple digits (less selective) (Besle et al., 2014; Martuzzi et al., 2014; Stringer et al., 2014). Recent 7 T work also showed that automatized vibrotactile stimulation induces lower BOLD responses over the entire S1 and in particular in BA 2 compared to manual stroking (van der Zwaag et al., 2015), a finding that may explain the difficulty of activating BA 2 representations in studies using automatized vibrotactile stimulation (Besle et al., 2014; Sanchez-Panchuelo et al., 2010; Stringer et al., 2011). Instead, manual stroking has been shown to induce reliable BOLD responses in BAs 3b, 1 and 2 (Martuzzi et al., 2014, 2015; van der Zwaag et al., 2015), although BA2 representations were again found to be smaller.

Most previous S1 studies have centered on the investigation of the hand area of S1, likely because of its large cortical representation and its important role in tactile perception (Martuzzi et al., 2014; Overduin and Servos, 2004; Sanchez-Panchuelo et al., 2010; Schweizer et al., 2008; Stringer et al., 2011; Weibull et al., 2008). Considering the importance of the legs and feet for stance, balance and locomotion, surprisingly few imaging studies investigated the representations of the lower limbs in human S1 (Bao et al., 2012; Nakagoshi et al., 2005; Saadon-Grosman et al., 2015). Nakagoshi et al. (2005) mapped the knee and ankle regions, Bao et al. (2012) mapped several leg regions. Both studies reported a lateral to medial organization when moving from proximal to more distal skin regions and reported the organization of the leg representation in S1 only at the group level (i.e. not for each subject individually). Recently, Saadon-Grosman et al. (2015) used whole-body somatotopic mapping in individual subjects (at 3 T) and reported a latero-medial gradient along S1 when moving from hip to toes. However, none of the aforementioned studies investigated lower limb representations within the different subregions of S1 separately at high spatial resolution.

The aim of the present study was to precisely map the S1 representations of six skin regions of the right lower limb and of the left lower limb in BAs 3b, 1, and 2, and to do this at the level of single subjects. To this aim, we first applied the mapping procedure proposed in Martuzzi et al. (2014) to three body regions on the foot (big toe, small toe, heel) and three body regions on the leg (calf, thigh and hip), separately for the right and the left lower extremities using tactile stimulation at ultra-high field 7 T fMRI. We first analyzed the location of each mapped representation and determined its strength and extent. We further investigated the selectivity of these representations across the different mapped body parts for each BA separately. For this, following the approach of Martuzzi et al. (2014), we determined for each mapped voxel in S1 to which degree it also respond to the stimulation of other body parts (in addition to the body part that was most strongly represented at that voxel). Finally, we conducted dissimilarity analysis to investigate whether the anatomical and functional properties of S1 leg representations reflect the physical structure of lower limbs (for detailed predictions see methods).

## Methods

### *Subjects*

15 healthy subjects (5 females) aged between 18 and 39 years old (mean±std: 24.3±5.2 years) participated in the study. One participant was excluded due to excessive motion during MRI acquisition (up to 5 mm of movement in the z-direction for this particular subject). All participants were right handed and had a right foot preference, as assessed during an oral interview adapted from the Edinburgh Handedness Inventory (Oldfield, 1971) (see ISM. 1).

All subjects gave written informed consent, all procedures were approved by the Ethics Committee of the Faculty of Biology and Medicine of the University of Lausanne, and the study was conducted in accordance with the Declaration of Helsinki.

### *Experimental procedure*

Subjects were scanned in supine position while tactile stimulation was delivered to the selected body parts on the lower limbs. Tactile stimulation consisted of a gentle manual stroking performed by an experimenter with his index finger, as a previous study showed that this stimulus induces more reliable BOLD signal responses over the different BAs (BA 3b, BA 1 and BA 2) forming S1, compared to vibrations or tapping (van der Zwaag et al., 2015). The experimenter was standing at the entrance of the bore to provide the stimulation and received instructions by means of MR compatible earphones. Six regions on both legs (big toe, small toe, heel, calf, thigh and hip) were repeatedly stimulated. During one run, the six regions of the same limb were stroked in a fixed order (thigh – big toe – calf – heel – hip – small toe) and the sequence was repeated 4 times. The order of the lower limb being stimulated was randomized across participants. Stimulation periods of 20 s were interleaved with periods of 10 s of rest (rest periods with no tactile stimulation). The skin regions were repeatedly stroked on the same portion of naked skin at an approximate rate of 1 Hz, corresponding to a surface of about 3 $cm^2$, with the exception of the small toe, which was stroked on its entire length (i.e. it was smaller than 3 $cm^2$). To reduce the variability of the tactile stimulation across participants and to guarantee that a reliable and constant pressure was exerted, the stroking was always performed by the same researcher, which received extensive training prior to data acquisition. To enquire about our participant's perception of the tactile stimulation, the participants were verbally asked between each run whether they could clearly feel the stimulation, if it was not the case the run would be repeated (this only happened on 7 occasions).

### *Data acquisition*

MR images were acquired using a short-bore head-only 7 T scanner (Siemens Medical, Germany) equipped with a 32-channel Tx/Rx RF-coil

(Nova Medical, USA) (Salomon et al., 2014). Functional images were acquired using a sinusoidal readout EPI sequence (Speck et al., 2008) and comprised 28 axial slices placed approximately orthogonal to the postcentral gyrus (in-plane resolution=1.3×1.3 $mm^2$, slice thickness=1.3 mm, no gap, TR=2 s, TE=27 ms, flip angle=75°, matrix size=160×160, FOV=210 mm, GRAPPA factor=2). The mapping sequence included 361 volumes for each of the lower limbs.

For each subject, a set of anatomical images was acquired using an MP2RAGE sequence (Marques et al., 2010) in order to facilitate the separation of Brodmann areas (BAs) and for display purposes (resolution=1×1x1$mm^3$, TE =2.63 ms, TR =7.2 ms, TI1=0.9 s, TI2 =3.2 s, $TR_{mprage}$ =5 s). To aid coregistration between the functional and the anatomical images, a whole brain EPI volume was also acquired with the same inclination used in the functional runs (81 slices, in-plane resolution=1.3×1.3 $mm^2$, slice thickness=1.3 mm, no gap, TE=27 ms, flip angle=75°, FOV=210 mm, GRAPPA factor=2).

*Data processing*

All images were analyzed using the SPM8 software (Wellcome Department of Cognitive Neurology, London, UK). The MRIcron software was used for visualizing results in 3D space (McCausland Center for Brain Imaging, University of South Carolina, US, http://www.mccauslandcenter.sc.edu/mricro/mricron) and BrainVoyager QX was used for surface visualization (Brain Innovation, Maastricht, Netherlands).

Preprocessing of fMRI data included slice timing correction, spatial realignment, and smoothing (FWHM=2 mm). A GLM analysis was carried out to estimate the response induced by the stimulation of the different body regions. The model included 6 regressors (one for each stroked region) convoluted with the hemodynamic response and with the corresponding first-order time derivatives, as well as the 6 rigid-body motion parameters as nuisance regressors. For each limb separately, a F-contrast across all conditions was computed to identify all the voxels activated by the stroking of at least one region. A t-contrast (against rest periods) was also computed for each stimulated region.

*Separation of S1 into BAs 3b, 1 and 2*

Probabilistic maps for the separation of the postcentral gyrus into BAs 3b, 1 and 2 (Geyer et al., 1999, 2000; Grefkes et al., 2001) were used to separate the 3 homologous representations of each region. For each subject, the probabilistic maps were back-projected onto their native space using standard procedures implemented in SPM8.

*Definition of somatosensory representations*

Independently for each limb, the clusters corresponding to the representations of each stimulated body region were delimited using an approach previously presented in Martuzzi et al. (2014). First, the active voxels in the F-contrast ($p<0.0001$ uncorrected) located within the contralateral postcentral gyrus were used as a S1 mask to identify all voxels responding to at least the stimulation of one body part. Then, based on a "winner takes all" approach, each voxel within the S1 mask was labeled as representing the body region demonstrating the highest t-score (against rest periods) for that particular voxel. The identified clusters were further divided into BAs 3b, 1 and 2 using the probabilistic maps described above.

This approach has the advantage of producing continuous and non-overlapping body maps, similarly to the approach of phase encoding used in retinotopic mapping studies (Olman et al., 2010), as well as in studies focusing on the somatosensory system (Sanchez-Panchuelo et al., 2012; Saadon-Grosman et al., 2015) or the motor system (Zeharia et al., 2015). One of the drawbacks of this approach is that it is possible that one or more body regions are not associated with any voxel, because stimulation of other body parts may elicit higher activity in all considered voxels, leading to missing representations. However, across all subjects, only 2.4 representations on average (±std:±3.3, range 0–9) were missing out of a total of 36 representations per subject. Small toe, calf and thigh representations accounted for 94% of these missing representations.

*Single subject data*

To emphasize the importance and relevance of single subject analysis, we report the identified S1 maps for 4 individual participants (and for all individuals in Supplementary materials). In addition, we analyzed for these 4 individuals the cortical volumes and response selectivity of body representations. The cortical volume is measured as the number of voxels within each representation normalized by the total number of voxels of the corresponding BA of the same hemisphere to account for inter-subject and inter-areal volumetric differences. The response selectivity is measured as the average BOLD response (beta values) within each representation during the stimulation of the different body regions, which allows to investigate whether the stimulation of a given body region also elicits activity in other S1 representations. These data are presented in Supplementary materials.

*Analysis of somatotopic sequence*

Within each identified body representation, the coordinates of the peak activation (maximum t-value) were extracted and transformed into MNI coordinates using SPM8. In case of a missing body representation, we considered the original t-contrast of that body part (against rest periods) used to define somatosensory representations (see above) and extracted the coordinates of the peak activation located in the corresponding BA, which were transformed into MNI coordinates. The average MNI coordinates of peak activations of each representation were calculated by averaging across subjects. To assess the presence of somatotopic ordering, a Principal Component Analysis (PCA) was first computed to determine the main axis of orientation (corresponding to the 1st principal component) along the MNI coordinates of peak activations of the 6 representations (big toe - small toe - heel - calf - thigh - hip) within each BA and for each individual subject. The PCA procedure allows the spatial remapping of the MNI coordinates along the axis explaining the most variance, which is suitable to investigate the ordering of S1 representations. The spatial distribution across participants of these transformed coordinates of peak activations is reported for each BA.

To statistically evaluate the ordering, we computed Page's trend tests (Page, 1963) on the transformed coordinates for each BA. Page's trend test is a non-parametric test based on data ranking that can assess the ordering of a set of independent variables. We assessed ordering based on the following sequence as hypothesized in the section "*Study hypotheses*" (see below): "big toe - small toe - heel - calf - thigh - hip". The statistical significance of the calculated L-statistic (the equivalent of the t-value for a *t*-test) was assessed using the tabulated values reported by Page (1963) for 6 variables and a sample size of 14: L=1078 for p=0.05, L=1098 for p=0.01 and L=1121 for p=0.001. In addition, we report the average value of L-statistics for 1000 random permutations of our data. We note that we also investigated the second principal component of the PCA.

As a confirmatory analysis, we computed the Euclidean distances between the representation of the big toe and all other representations in each BA to assess whether the distance was increasing between representations as expected by the proposed ordering: "big toe - small toe - heel - calf - thigh – hip". The Euclidean distances were quantified using Page's trend tests (Page, 1963) as previously described for the ordering along the first principal component (values for statistical significance with 5 variables and 14 samples: L=661 for p=0.05, L=674 for p=0.01 and L=689 for p=0.001).

Additional analyses regarding the somatotopy of foot representations and the somatotopy of leg representations are provided in Supplementary materials.

*Analysis of somatotopic selectivity*

To investigate the somatotopic selectivity of the mapped representations, we computed the average BOLD response (beta values) within each representation during the stimulation of all other body regions. This measures the degree to which a given body representation can be co-activated by the stimulation of any other body region. We computed one-sample *t*-tests to assess whether the stimulation of other body regions could induce significant BOLD response within the dominant body region mapped to this S1 location. To account for multiple comparisons and find an appropriate statistical threshold, we used permutation tests. The beta values were randomly permuted and one-sample *t*-tests were computed. This procedure was repeated 1000 times. The resulting t-values were then sorted and the 95th percentile was selected as the statistical threshold, corresponding to $\alpha=0.05$ corrected (t-value=3.17). In case of a missing body representation data from that body representation were excluded from the analysis. This analysis was conducted in the native space of individual subjects.

To further investigate whether the observed patterns of somatotopic selectivity could be merely explained by the cortical distance between representations, we performed univariate regression analysis. We considered 3 different fitting functions: 1) a decaying linear function to describe a constant decrease in strength of co-activation with increased cortical distance, 2) a decaying exponential function to describe that co-activation decreases faster with increased cortical distance compared to the linear function (i.e. penalizing distant interactions), 3) a sigmoidal function to describe a functional clustering with local co-activations and a drastic decrease in strength of co-activation for distant interactions. Separately for each stimulated body region, each BA and each subject, we fitted the linear, exponential and sigmoidal functions to the data using the co-activations as the dependent variable and the cortical distance as the independent variable. Each of the fitting functions included 2 free parameters (slope and offset), which were optimized using a least-square approach. The best fitting function was determined by comparing the coefficient of determination $R^2$ using non-parametric Wilcoxon signed-rank tests with a Bonferroni correction (Wilcoxon, 1946). Unreliable regressions ($R^2<0.3$) were excluded from the pairwise comparisons. We note that the fitting parameters of the best fitting function were further analyzed to investigate possible differences across body representations, BAs and hemispheres using linear mixed models on the ranked data (Cnaan et al., 1997).

*Analysis of extent and strength of BOLD activations*

To investigate differences across body representations, BAs and hemispheres in terms of extent and strength of BOLD activations associated with the stimulation of the different body parts, we conducted the following analyses.

First, we analyzed the extent of BOLD activations using the size of each cortical representation as dependent variable. The volume in $mm^3$ of each representation was computed, and normalized by the total volume of the corresponding BA of the same hemisphere to account for inter-subject and inter-areal volumetric differences. We note that this represents a relative volume, and not an absolute volume, measuring the fraction occupied by a given body representation in each area. In case of a missing body representation, the cortical volume was set to 0. We computed a three-way repeated-measures ANOVA with body region (6 levels), BA (3 levels), and hemisphere (2 levels) as within-subject factors.

Second, we investigated the strength of BOLD activations using the peak activation within each representation as dependent variable. In case of a missing body representation, the peak activation located in the corresponding BA was extracted from the original t-contrast (against rest) of that body part. Similarly to the previous analyses, we computed a three-way repeated-measures ANOVA with body region (6 levels), BA (3 levels), and hemisphere (2 levels) as within-subject factors.

For both analyses, post-hoc Bonferroni corrected pair-wise comparisons were used to assess differences between levels of significant factors. The significance level was set to $\alpha=0.05$ for both ANOVAs and post-hoc tests. We also assessed the sphericity and the normality of the data. In case of violation of sphericity, we conducted a Greenhouse-Geisser correction on the ANOVA (Geisser and Greenhouse, 1958). In case of violation of normality as assessed by the Kolmogorov-Smirnov test (Govindarajulu, 1976), we computed a confirmatory analysis using linear mixed models with the ranked data as dependent variable (Cnaan et al., 1997). Both analyses of extent and strength of BOLD activations were conducted in the native space of individual subjects.

*Dissimilarity analysis*

The goal of dissimilarity analysis was to investigate whether the different properties of S1 representations are related to the physical structure of lower limbs. To this end, we computed dissimilarity matrices based on: 1) the peak locations of S1 representations 2) the co-activations between S1 representations (average pair-wise co-activation) and 3) the representational similarity of S1 representations (Representational Similarity Analysis, RSA, Kriegeskorte et al., 2008). As control measures, we computed dissimilarity matrices based on the differential volume of activation between pairs of S1 representations and the differential strength of activation between pairs of S1 representations. This procedure was carried out separately for each BA and each participant.

The "peak location" dissimilarity between pairs of S1 representations was computed as the Euclidean distance between the cortical locations of S1 representations and was derived from the analyses presented in section *Analysis of somatotopic sequence*.

The "co-activation" dissimilarity between pairs of S1 representations was computed using the patterns of co-activations and was derived from the analyses presented in section *Analysis of somatotopic selectivity*. The co-activations between pairs of S1 representations are used as a measure of similarity, i.e. pairs of S1 representations are considered similar if they are reciprocally co-activated when stimulated separately. The non-symmetrical matrices of co-activations were transformed into symmetrical dissimilarity measures as described in ISM.2.

The "RSA" dissimilarity was computed using RSA. We compared the multi-voxel patterns of S1 activations associated with the stimulation of the different parts of the lower limbs. First, a GLM analysis was computed to estimate the beta parameters associated with each period of tactile stimulation. Second, the dissimilarity between each pair of S1 representations was computed as the cross-validated mahalanobis distance (Nili et al., 2014) between the activation patterns extracted from the GLM.

As controls, we computed dissimilarity measures between each pair of S1 representation based on the differential volume of activation ("Δ volume") and the differential strength of activation ("Δ strength") derived from analyses presented in section *Analysis of extent and strength of BOLD activations*.

These 5 measures of dissimilarity ("peak locations", "co-activations", "RSA", "Δ volume" and "Δ strength") were compared to a theoretical model of dissimilarity based on the physical structure of lower limbs (Contini, 1972). The pair-wise distances between each pair of body parts were expressed as a fraction of total height. Separate models for male and female participants were considered (see ISM.3). The matrices associated with the 5 measures of dissimilarity were correlated with the matrix associated with the theoretical model of dissimilarity separately for each BA and each participant (upper part of the matrices were treated as data vectors). The resulting correlation values were normalized using Fischer transformations and statistically analyzed using a three-way repeated-measures ANOVA with dissimilarity measure (5 levels), BA (3 levels), and side (2 levels) as within-subject factors. Post-hoc Bonferroni corrected pair-wise comparisons were used to assess differences between levels of significant factors. As for previous analyses, the significance level was set to $\alpha=0.05$ for both the ANOVA and post-hoc tests. We also assessed the sphericity and the normality of the data. In case of violation

of sphericity, we conducted a Greenhouse-Geisser correction on the ANOVA (Geisser and Greenhouse, 1958). In case of violation of normality as assessed by the Kolmogorov-Smirnov test (Govindarajulu, 1976), we computed a confirmatory analysis using linear mixed models with the ranked data as dependent variable (Cnaan et al., 1997).

For display purposes, we used classical multidimensional scaling (also known as Principal Coordinate Analysis, Seber, 1984) to represent the dissimilarity measures on a 2D planar layout.

### *Study hypotheses*

Based on the work by Penfield and colleagues (Penfield and Boldrey, 1937; Rasmussen and Penfield, 1947) and more recent neuroimaging work (Bao et al., 2012; Nakagoshi et al., 2005; Saadon-Grosman et al., 2015, see also Zeharia et al. (2015) for related work on movement representations in M1 mapping), we expected the toes to be located contralaterally in the most medial and superior portion of the postcentral gyrus, and more proximal foot and leg representations to be located more laterally on the postcentral gyrus. We also expected (by homology with the upper limb digits) that the big toe (digit I) would be located more medially compared to the small toe (digit V). Thus, we expect that lower limb representations would follow a medial to lateral gradient from big toe to hip ("big toe - small toe - heel - calf - thigh - hip"). We also quantified the extent and strength of BOLD responses of each mapped foot and leg representation in the different BAs of each individual subject, and investigated the selectivity of each mapped representation across the different BAs. These metrics were analyzed to investigate differences across body regions, across BAs and across hemispheres. We expected that the extent and strength of BOLD responses associated with big toe representation would be enhanced compared to small toe representation, in line with what was previously shown for the corresponding digits of the hand (Martuzzi et al., 2014). Furthermore, we also expected that the size of representations within BA 2 would be smaller in comparison to BA 3b and BA 1 as previously reported for finger representations by studies using natural stimulation (Martuzzi et al., 2014, 2015; van der Zwaag et al., 2015). We also searched for potential differences across hemispheres in favor of asymmetric S1 activations in our right-footed participants. In addition, we hypothesized that human BA 2, which has the largest receptive fields in S1 of non-human primates (Costanzo and Gardner, 1980; Gardner, 1988), would show less selectivity in response to tactile stimulation of different leg and foot regions compared to other BAs, as already shown for finger representations in human S1 by recent work (Besle et al., 2014; Martuzzi et al., 2014; Stringer et al., 2014). Finally, regarding dissimilarity analysis, we expected that the theoretical model based on the physical structure of the lower limbs would correlate with the anatomical ("peak locations") and functional ("co-activations" and "RSA") dissimilarity measures, but not with the control dissimilarity measures ("Δ volume" and "Δ strength").

## Results

A total of 12 body regions (6 on each body side) were stimulated during the acquisition of functional data, allowing the mapping of the cortical representations of these body regions within 3 different BAs (BA 3b, BA 1 and BA 2) as defined by published probabilistic maps (Geyer et al., 1999, 2000; Grefkes et al., 2001) leading to a total of 36 mapped representations in S1 per subject (see Methods).

### *Somatotopic sequence*

The S1 maps of 4 representative subjects are shown in Fig. 1 (see ISM.4 and ISM.5 for all subjects). Additional data regarding the properties of these individual maps are presented in Supplementary materials. In all participants, lower limb representations were located in the superior part of the postcentral gyrus. Within the identified clusters, leg representations were located laterally and foot representations medially in all BAs. This was the case for the large majority of participants (only in one subject, subject 7, this pattern was not present). Moreover, this result was statistically confirmed by the comparison between the locations of peak activations along the first principal component for average foot representations (average of big toe, small toe and heel) and average leg representations (average of calf, thigh and hip) (see Supplementary materials).

The average MNI locations of peak activations of all mapped representations are reported in Table 1 and shown in Fig. 2. Similarly to what was described for individual subjects (see Supplementary materials), the foot representations were located in the medial region of the postcentral gyrus in the hemisphere contralateral to the stimulated foot and located more medially with respect to leg representations. The calf, thigh and hip representations were located most laterally and appeared in an orderly manner moving from medial to lateral positions, respectively (all representations were lateral with respect to the foot representations). However, there was no consistent ordering of foot representations across BAs.

The spatial distributions across participants of locations of peak activations within each BA along the first principal component are shown in ISM.6. Using these transformed coordinates as dependent variables (Page's trend tests), we found that the somatotopic sequence of "big toe - small toe - heel - calf - thigh - hip" led to statistically significant ordering in all tested BAs (all $p<0.001$). The same tests performed with random permutations did not lead to significant results (Table 2A). The same analysis performed with the 2nd principal component did not lead to any systematic ordering across foot or leg representations. We further analyzed these data separately for foot and leg representations and found that a reliable somatotopic ordering was only present for the leg representations, but not for the foot representations (see Supplementary materials). Despite the partial evidence for somatotopic ordering across participants, we also found substantial overlap across the different distributions of locations of peak activations along the first principal component, suggesting a large degree of inter-subject variability. Indeed, on average only 2.2 out of 14 subjects (6 at best) shared the same representation at a given voxel.

Euclidean distances between the representation of the big toe and all other representations for each BA are shown in ISM.7. Page's trend tests (Tab.2B) showed that the distances between the representation of the big toe and other lower limb representations were significantly increasing in all BAs as expected by the proposed ordering (big toe - small toe - heel - calf - thigh – hip), thus confirming our previous result (all $p<0.05$).

To summarize, we were able to quantify somatotopy for each BA, in particular for calf, thigh and hip representations, which appeared somatotopically organized in S1 subregions. The foot representations were located more medially compared to leg representations, but did not appear in a consistent ordering along S1. Moreover, despite this somatotopic ordering across participants, the exact spatial layout of somatotopy strongly differed across subjects.

### *Somatotopic selectivity*

S1 voxels were linked to a certain body part depending on which body part most strongly activated a given voxel (see section 2.6 of methods). Here, we tested for each stimulated body region whether the tactile stimulation led to statistically significant positive BOLD responses within any of the other mapped representations (corrected for multiple comparisons, see Methods). Determining the somatotopic selectivity of the 6 mapped body regions within the different BAs in right and left S1 (Fig. 3), we found that stimulation of big and small toes never activated leg representations (calf - thigh - hip) and that stimulation of leg representations never activated foot representations (big toe - small toe - heel). We observed patterns of co-activation for each of the three foot representations (big toe, small toe, and heel) in all BAs of both hemispheres: stimulation of the big toe strongly co-activated the small toe and heel representations in all BAs (except for the heel in right BA 2). Stimulation

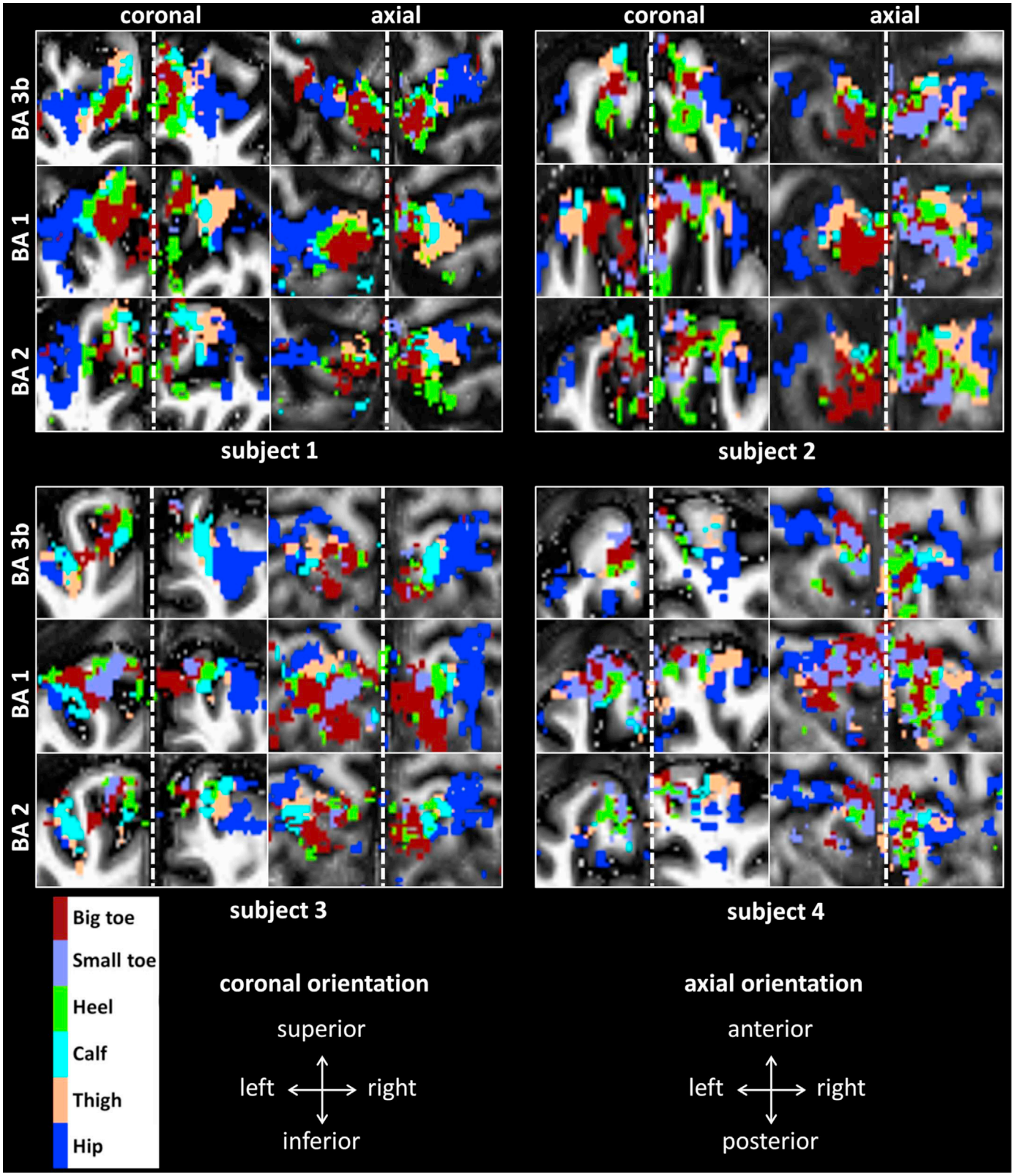


**Fig. 1.** Individual S1 maps. Somatosensory representations within BA 3b, BA 1 and BA 2 of right and left big toe, small toe, heel, calf, thigh and hip of 4 individual subjects are shown. The maps are color-coded and represented on coronal and axial projections in native space of individual subjects (the projection of the maps lead to the apparent spatial overlap across BA's). The dashed line shows the separation between left and right hemispheres. Individual metrics for these subjects (cortical volume and somatotopic selectivity between representations, Fig. S1-S2) and S1 maps for all participants are presented in Figs. S3 and S4 in Supplementary materials.

**Table 1**
MNI Locations of peak activations. The location in MNI stereotaxic space of the average peak activations (mean±std) of the mapped representations in different BAs are reported for right body regions (top) and left body regions (bottom).

| | left hemisphere | | | | | | | | |
|---|---|---|---|---|---|---|---|---|---|
| | BA3b | | | BA1 | | | BA2 | | |
| | x | y | z | x | y | z | x | y | z |
| **big toe** | −8.2±0.7 | −42.0±1.3 | 65.7±1.2 | −8.8±1.4 | −39.9±1.5 | 67.0±1.5 | −9.4±1.1 | −41.2±1.4 | 66.9±1.1 |
| **small toe** | −8.8±1.0 | −42.2±1.4 | 65.0±1.3 | −9.2±2.1 | −37.8±1.9 | 65.9±1.7 | −7.2±1.2 | −41.4±1.7 | 65.2±1.4 |
| **heel** | −8.6±0.8 | −42.6±1.5 | 64.4±1.2 | −10.0±1.7 | −41.9±1.5 | 68.6±1.7 | −8.7±1.3 | −42.4±1.4 | 64.5±1.3 |
| **calf** | −12.5±2.1 | −41.8±1.6 | 62.3±2.3 | −14.5±1.6 | −39.5±1.2 | 68.8±1.5 | −13.1±2.5 | −43.9±2.3 | 62.5±4.0 |
| **thigh** | −14.2±1.6 | −38.7±1.5 | 64.8±1.6 | −17.4±1.1 | −37.9±1.1 | 69.0±1.5 | −15.4±1.8 | −38.3±1.6 | 66.3±1.7 |
| **hip** | −22.3±1.6 | −37.7±1.1 | 57.1±1.5 | −21.1±1.1 | −38.8±1.0 | 64.3±1.9 | −20.3±1.6 | −39.3±1.0 | 60.0±1.7 |
| | **right hemisphere** | | | | | | | | |
| | BA3b | | | BA1 | | | BA2 | | |
| | x | y | z | x | y | z | x | y | z |
| **big toe** | 8.2±1.0 | −39.8±2.1 | 67.8±1.0 | 11.7±2.0 | −42.1±2.3 | 70.9±1.0 | 9.9±1.4 | −39.3±1.5 | 70.1±0.8 |
| **small toe** | 9.2±2.5 | −39.1±2.0 | 65.4±2.7 | 8.0±1.7 | −37.9±1.2 | 70.7±1.8 | 6.6±1.3 | −39.1±1.4 | 68.2±1.6 |
| **heel** | 10.1±1.5 | −42.1±1.4 | 67.0±1.3 | 10.2±1.8 | −39.6±1.6 | 68.5±1.5 | 11.2±1.9 | −41.5±1.7 | 67.6±1.6 |
| **calf** | 12.7±2.2 | −38.1±2.0 | 66.0±2.9 | 15.1±1.5 | −42.4±2.4 | 69.1±1.2 | 15.1±2.8 | −40.4±2.1 | 64.7±3.2 |
| **thigh** | 15.2±2.2 | −40.5±1.8 | 62.9±1.3 | 18.1±1.1 | −39.3±1.4 | 68.9±1.4 | 17.6±1.1 | −38.0±1.2 | 67.1±1.2 |
| **hip** | 20.7±1.5 | −37.0±1.7 | 59.5±1.8 | 22.6±1.2 | −39.2±1.2 | 66.1±1.6 | 20.9±1.2 | −38.4±1.1 | 61.5±1.7 |

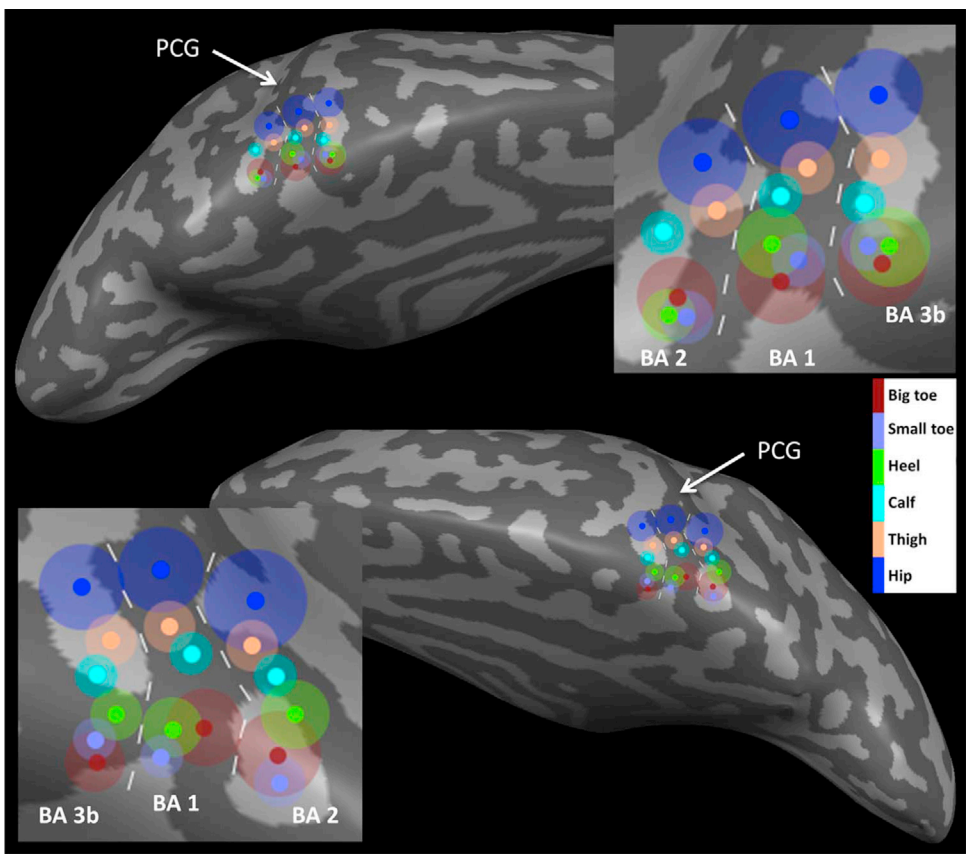


**Fig. 2.** Locations of lower limb representations. Average MNI locations of peak activations are shown on an inflated brain. The somatosensory representations of right (top) and left (bottom) lower limbs within BAs 3b, 1 and 2 (big toe, small toe, heel, calf, thigh and hip) are shown with color-coded circles. The transparent circles represent the respective size of each representation. The postcentral gyrus (PCG) is indicated by the white arrows.

of the small toe strongly co-activated the big toe and heel representations in all BAs. Concerning the stimulation of the heel, which strongly co-activated big toe and small toe representations, the co-activations also involved the calf representations (broader *within* limb selectivity). *Within* limb somatotopic selectivity was reduced for calf, thigh and hip stimulation. In particular, calf stimulation (right and left) either co-activated exclusively thigh representations or did not elicit any co-activations (left BA 2). Thigh stimulation either co-activated calf and hip representations or did not induce any co-activations (left BA 3b and left BA 2). Finally, hip stimulation either exclusively co-activated thigh representations or did not elicit any co-activation (left BA 3b and left BA 2). We note that there was no evidence of qualitative differences in somatotopic selectivity across BAs.

To further investigate whether the lack of functional interactions between foot and leg representations could be explained by the factor of cortical distance, we conducted regression analysis to characterize the

**Table 2**
Summary of Page's Trend tests. L statistics and corresponding p-values are reported for the tested ordering: "big toe - small toe - heel - calf - thigh - hip". In addition, we report the average L statistics for random permutations (n=1000) of our data. In the top panel, we report the page tests performed on transformed coordinates along the first principal component within each BA. Values for statistical significance were derived from Page (1963) for data with 6 variables and 14 samples (L=1078 for p=0.05, L=1098 for p=0.01 and L=1121 for p=0.001). In the bottom panel, we report the page tests performed on the Euclidean distances between big toe representation and the other representations within in each BA. Values for statistical significance were derived from Page (1963) for data with 5 variables and 14 samples (L=661 for p=0.05, L=674 for p=0.01 and L=689 for p=0.001).

| | Somatotopic | | Random | |
|---|---|---|---|---|
| | **L statistic** | **p-value** | **L statistic** | **p-value** |
| **left BA 3b** | 1193 | p<0.001 | 1027 | p=0.48 |
| **left BA 1** | 1128 | p<0.001 | 1032 | p=0.50 |
| **left BA 2** | 1189 | p<0.001 | 1028 | p=0.48 |
| **right BA 3b** | 1187 | p<0.001 | 1028 | p=0.49 |
| **right BA 1** | 1180 | p<0.001 | 1030 | p=0.50 |
| **right BA 2** | 1168 | p<0.001 | 1029 | p=0.50 |
| | **Somatotopic** | | **Random** | |
| | **L statistic** | **p-value** | **L statistic** | **p-value** |
| **left BA 3b** | 748 | p<0.001 | 630 | p=0.49 |
| **left BA 1** | 703 | p<0.001 | 630 | p=0.50 |
| **left BA 2** | 710 | p<0.001 | 630 | p=0.49 |
| **right BA 3b** | 718 | p<0.001 | 630 | p=0.48 |
| **right BA 1** | 685 | p<0.01 | 630 | p=0.49 |
| **right BA 2** | 663 | p<0.05 | 631 | p=0.49 |

relationship between co-activations and cortical distance. Univariate regression analysis (separately for each stimulated body region, each BA and each participant) was done to determine which regression function (linear, exponential or sigmoidal) best describes the relationship between co-activations and cortical distance. Computing pairwise Wilcoxon signed-rank tests (Bonferroni corrected) revealed that the sigmoidal fitting function performed better compared to the linear and exponential fitting functions (mean±std: linear fit R2=0.64±0.18, exponential fit $R^2$=0.69±.019, sigmoidal fit R2=0.74±0.19; linear vs sigmoidal: $Z_{366}$=12.8, p<0.001; exponential vs sigmoidal: $Z_{378}$=4.7, p<0.001). Analysis of the parameters (slope, offset) of the sigmoidal regression revealed no significant differences with respect to body regions, BAs or side.

Finally, we analyzed *between* limb somatotopic selectivity (i.e. does stimulation of a body region lead to significant responses in the hemisphere ipsilateral to the stimulated body region). Stimulation of all body regions (except the hip) induced no BOLD response or a negative BOLD response in ipsilateral S1 representations. Only hip representations were co-activated bilaterally during tactile stimulation of the hip in all BAs (right and left) (ISM.8).

To summarize, we found that *within* limb somatotopic selectivity was weaker for the three tested foot regions compared to the three tested leg regions. In addition, there were no co-activations between toe and leg representations. This effect was associated with differences in cortical distance and followed a sigmoidal shape. There was no evidence in favor of differences in somatotopic selectivity between the different BAs. The hip was the only body region, which elicited significant bilateral activations.

### *Extent and strength of BOLD activations*

In order to compare the extent and strength of BOLD activations within the cortical representation of each of the 6 mapped body regions within the different BAs in right and left S1, we analyzed the cortical volume and peak activation within each of the 36 mapped body representations (three-way repeated measures ANOVAs with body region, BA, and hemisphere as within subject factors).

For the analysis of cortical volume, the ANOVA showed a significant main effect of body region ($F_{5,65}$=25.3, p<0.001, Fig. 4A). Post-hoc Bonferroni corrected comparisons revealed that the big toe representations (independent of BA or hemisphere) had a significantly larger volume than those of the small toe, calf and the thigh (all p<0.001). Furthermore, we found that the hip representation had a significantly larger volume than the small toe, heel, calf and thigh representations (all p<0.001). This analysis also revealed that the heel representation had a significantly larger volume than those of the small toe and the calf (p=0.02 and p=0.002 respectively). There was also a main effect of BA ($F_{2,26}$=13.2, p<0.001, Fig. 4B), indicating that the volume of body representations differed across BAs. Post-hoc Bonferroni corrected comparisons showed that the volumes of representations within BA 2 were smaller compared to BA 3b and BA 1 (p<0.001 and p=0.008 respectively). There were no significant interactions (all p>0.07). We note that the normality of cortical volume data was not fully satisfied. Therefore, we replicated the analysis using linear mixed models on the ranked data, confirming our results.

For peak activations, the ANOVA showed a significant main effect of body region ($F_{5,65}$=23.7, p<0.001, Fig. 5A). Post-hoc pairwise comparisons (Bonferroni corrected) revealed that the big toe representations (independent of BA or hemisphere) had significantly greater peak activations than those of the small toe, calf and the thigh (all p<0.001). Furthermore, we found that the hip representations had significantly greater peak activations than those of small toe, calf and thigh (p<0.001, p<0.001 and p=0.01 respectively). This analysis also revealed that the heel representations had significantly greater peak activations than small toe, calf and thigh (p=0.002 and p<0.001 and p=0.02 respectively). Overall, this shows that certain body parts, especially big toe (but also heel and hip), were associated with greater peak activations compared to other body parts, and that this effect was present in all tested BAs and in both hemispheres. We also found a main effect of BA ($F_{2,26}$=6.3, p=0.01, Fig. 5B) indicating that peak activations within body representations differed across BAs independently from the body part represented and independently from the hemisphere. Post-hoc pairwise comparisons (Bonferroni corrected) showed that peak activations within BA 3b were weaker compared to BA 1 (p=0.005) without any other significant differences. A significant two-way interaction between body region and side was found ($F_{5,65}$=4.5, p=0.006). There was no difference between mapped body representations in the left versus right hemisphere (i.e. larger left S1 big toe representation versus right S1 big toe representation). Instead the body region x side interaction was driven by greater peak activations for right foot representations in the left hemisphere compared to left foot representations in the right hemisphere and by greater peak activations for right leg representations in the left hemisphere compared to left leg representations in the right hemisphere (although the post-hoc pairwise comparisons were not significant). Finally, a two-way interaction between BA and side was also found ($F_{2,26}$=4.9, p=0.03) and post-hoc pairwise comparisons (Bonferroni corrected) showed that peak activations within BA 3b are greater in the right hemisphere compared to the left hemisphere (p=0.03).

To summarize, our results indicate that in right-footed individuals overall the big toe representation is associated with stronger and larger BOLD responses than the small toe representation. This was also the case for hip representations compared to other leg representations. There were no differences in right versus left S1 activations for any of the mapped body regions.

### *Dissimilarity analysis*

Here we investigated whether the different measures of dissimilarity ("peak locations", "co-activations", "RSA", "Δ volume" and "Δ strength") were related to the physical structure of lower limbs. Data averaged across all BAs are represented in Fig. 6 (and in Fig.S3–S8 separately for each BA), where the different dissimilarity measures are shown along with the corresponding 2D configuration based on multidimensional scaling. We expected that dissimilarity measures based on "peak locations", on "co-activations", and on "RSA" would be organized into a

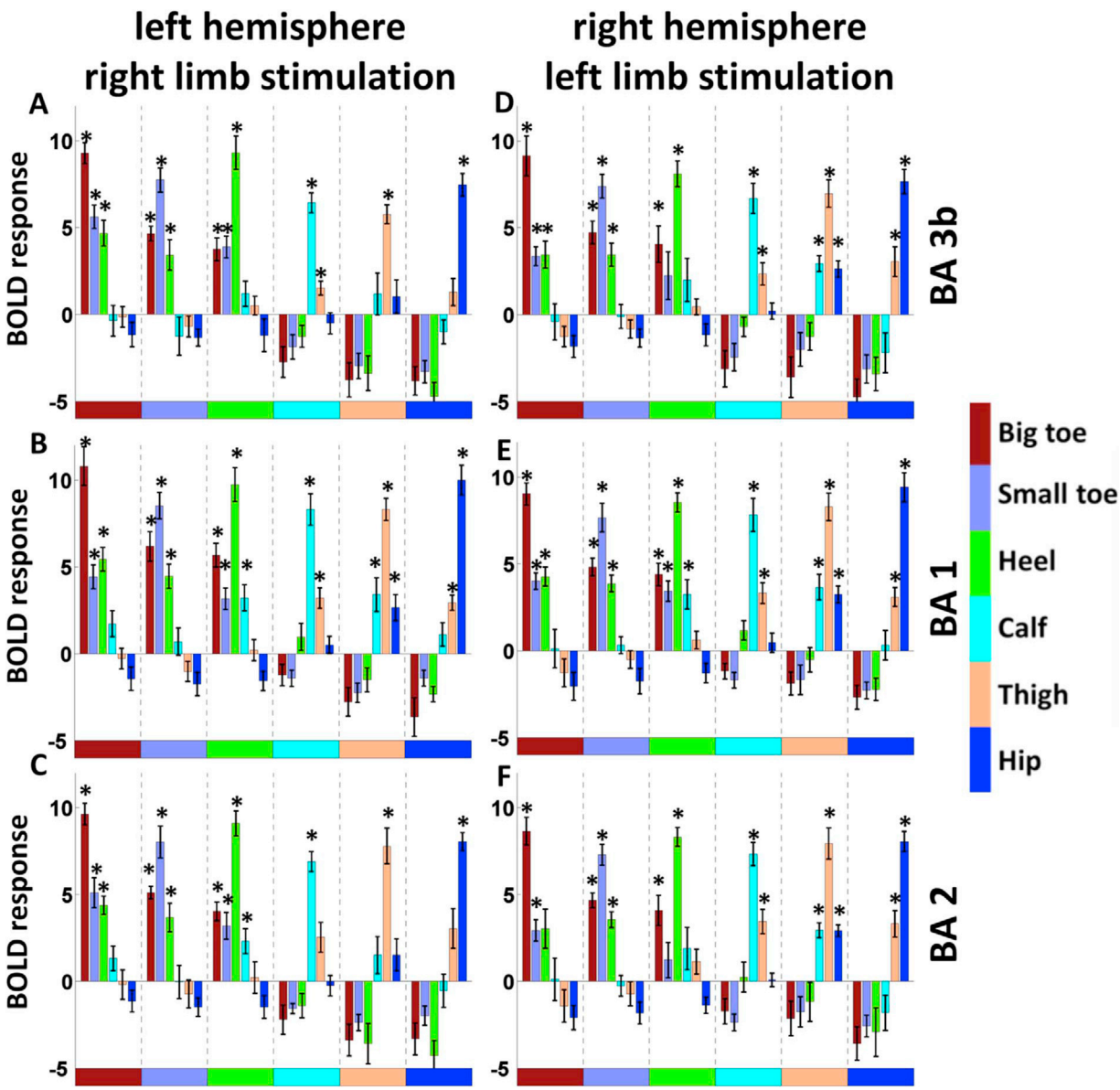


**Fig. 3.** *Within* limb somatotopic selectivity in lower limb representations in different BAs and hemispheres. The mean BOLD activations within the mapped representations are plotted and color-coded. On the horizontal axis, data are grouped by stimulated body regions. Panels a and d show the representations within BA 3b for left and right hemisphere respectively. Panels b and e show the representations within BA 1 for left and right hemisphere, respectively. Panels c and f show the representations within BA 2 for left and right hemisphere, respectively. Error bars represent standard errors of the mean. Asterisks represent significant BOLD activations as defined by permutation tests (see *Methods* for details).

somatotopic configuration, meaning that a low dissimilarity would be found between body parts located closely to each other on the body.

Qualitatively, we observed a somatotopic configuration for the dissimilarity measures based on "peak locations" (Fig. 6A), on "co-activations" (Fig. 6B), and on "RSA" (Fig. 6C). This was not the case for dissimilarity based on volume of activation (Fig. 6D) or strength of activation (Fig. 6E). This was found for each BA (see Fig.S4–S9). To statistically quantify this effect, we compared the different measures of dissimilarity with a theoretical model of the physical structure of lower limbs (Fig. 6F) derived from the work of Contini (1972). The correlations between the dissimilarity measures and the theoretical model were analyzed by means of a three-way repeated measures ANOVA with dissimilarity measure, BA, and side as within subject factors. The ANOVA showed a significant main effect of dissimilarity measure ($F_{4,40}$=155.2, $p<0.001$, Fig. 6G). Post-hoc Bonferroni corrected comparisons revealed that the dissimilarity measures based on "peak locations", "co-activations" and "RSA" were significantly more correlated with the theoretical model compared to the dissimilarity measures based on volume of activation ("Δ volume") and strength of activation ("Δ strength") (all $p<0.001$). In addition, the dissimilarity measures based on "co-activations" and "RSA" better correlated with the theoretical model compared to the dissimilarity measure based on "peak lcoations" (all $p<0.001$). There were no other significant main effects or interactions (all $p>0.06$). As the normality of these data was not guaranteed, we replicated the analysis using linear mixed models on the ranked data, confirming our results.

To summarize, dissimilarity analysis showed that the properties of S1 representations ("peak locations", "co-activations" and "RSA") reflect the physical structure of lower limbs. This was particularly the case for the functional properties of S1 ("co-activations" and "RSA").

## Discussion

The present work investigated the foot and leg representation in human S1. By stimulating six different body regions on each side of the body during the acquisition of fMRI data at ultra-high field, we were able

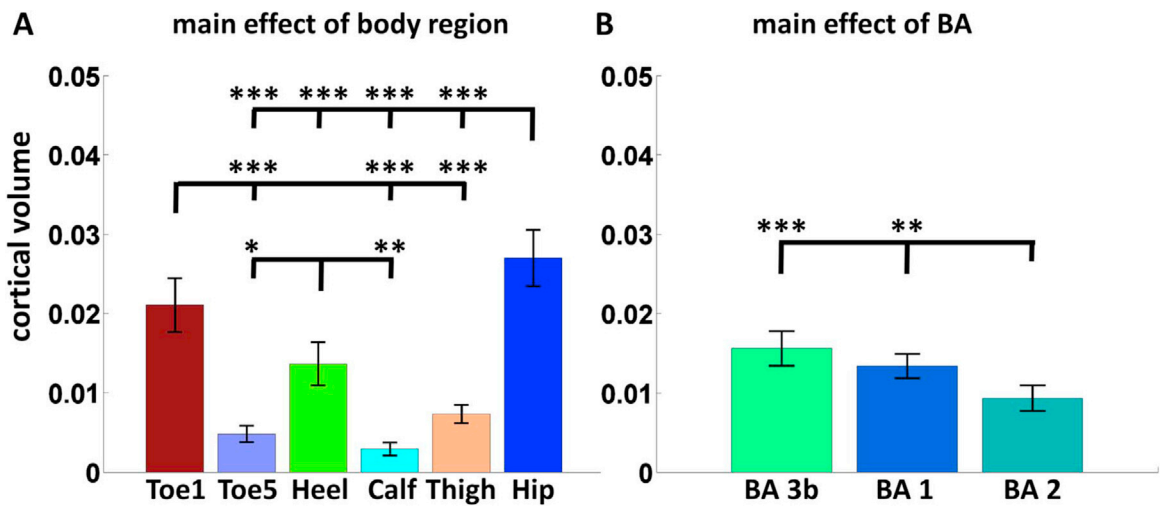


**Fig. 4.** Extent of BOLD activations. a) Main effect of body regions for the analysis of cortical volume ($F_{5,65}$=25.3, p<0.001). In the legend, "Toe1″ stands for big toe and "Toe5″ stands for small toe. b) Main effect of BA for the analysis of cortical volumes ($F_{2,26}$=13.2, p<0.001). The results are presented in the color-coded bar plot. Error bars represent standard errors of the mean. Significant post-hoc comparisons between the respective volumes of body representations are shown with asterisks (* p<0.05, ** p<0.01, *** p<0.001).

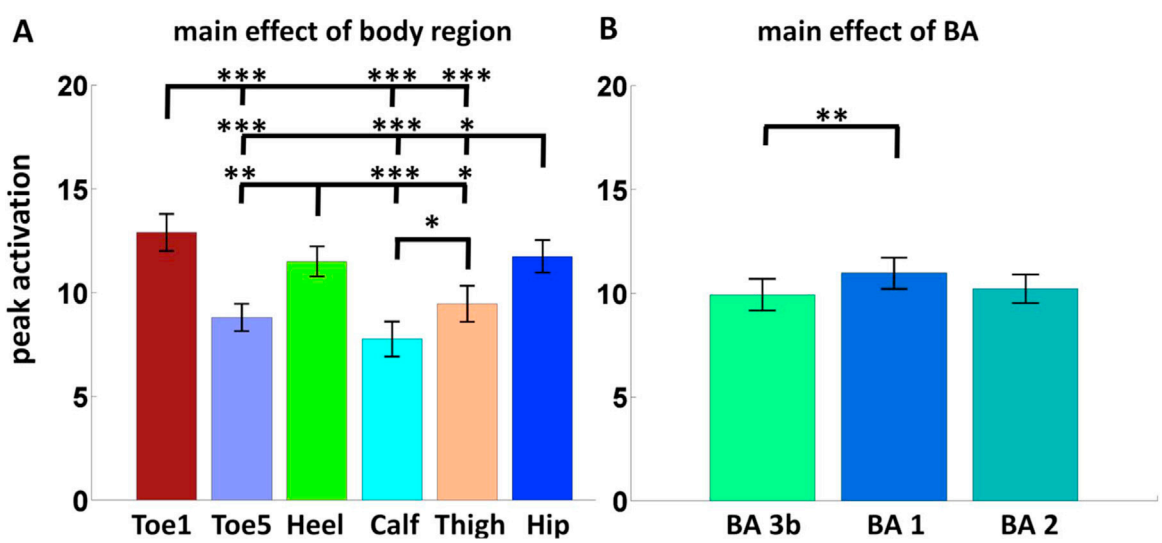


**Fig. 5.** Strength of BOLD activations. a) Main effect of body regions for the analysis of peak activations ($F_{5,65}$=23.7, p<0.001). In the legend, "Toe1″ stands for big toe and "Toe5″ stands for small toe. b) Main effect of BA for the analysis of peak activations ($F_{2,26}$=6.3, p=0.01). The results are presented in the color-coded bar plot. Error bars represent standard errors of the mean. Significant post-hoc comparisons between the respective peak activations within the different body representations are shown with asterisks (* p<0.05, ** p<0.01, *** p<0.001).

to identify separate representations for all body regions within three BAs of human S1, namely BA 3b, 1 and 2. A total of 36 (6 body regions, 3 BAs, 2 hemispheres) separate S1 lower limb representations were identified in each participant (with few exceptions), the sequence of which showed strong inter-subject variability. To the best of our knowledge, this is the first study characterizing the anatomical and functional properties of the representations of foot and leg in 3 different BAs in human S1, analyzing the somatotopic sequence, the extent and strength of BOLD responses and the somatotopic selectivity for the lower limb.

### *Anatomical location of S1 representations and inter-subject variability in the somatotopic sequence*

We report that the representation of the lower limb in S1 follows a medial-to-lateral gradient (when moving from distal to proximal parts of the lower limb) along the postcentral gyrus in BAs 3b, 1 and 2, partly reminiscent of the classic homunculus described in S1 (Bao et al., 2012; Nakagoshi et al., 2005; Penfield and Boldrey, 1937; Rasmussen and Penfield, 1947; Saadon-Grosman et al., 2015). However, this was only found for the leg representations (calf, thigh, hip) and in all investigated BAs, but was not the case for the foot representations. Our data are thus suggestive of a difference in foot versus leg representations in S1 (present data) and in foot versus hand representations in S1, with the different fingers ordered along the latero-medial axis (Martuzzi et al., 2014) whereas the toes are possibly ordered along the rostral-caudal axis in the postcentral gyrus (present data). This difference may be comparable with previous studies in non-human primates reporting differences regarding the organization of the digits of lower and upper limbs. Indeed, in monkey BA 3b, the lower limb digits have been reported to be organized along the latero-medial axis, while in monkey BA 1, they are rather organized along the rostro-caudal axis within a strip of the postcentral gyrus. Concerning upper limb digits, they have been reported to be somatotopically organized along the latero-medial axis of the postcentral gyrus in both monkey BA 3b and BA 1 and thus seem organized similarly with respect to human S1 (Merzenich et al., 1978; Kaas et al., 1979; Nelson et al., 1980; Martuzzi et al., 2014). Future studies will be necessary to investigate the representations of all 5 toes for more accurate mapping of toe somatotopy (not investigated in the present study; see

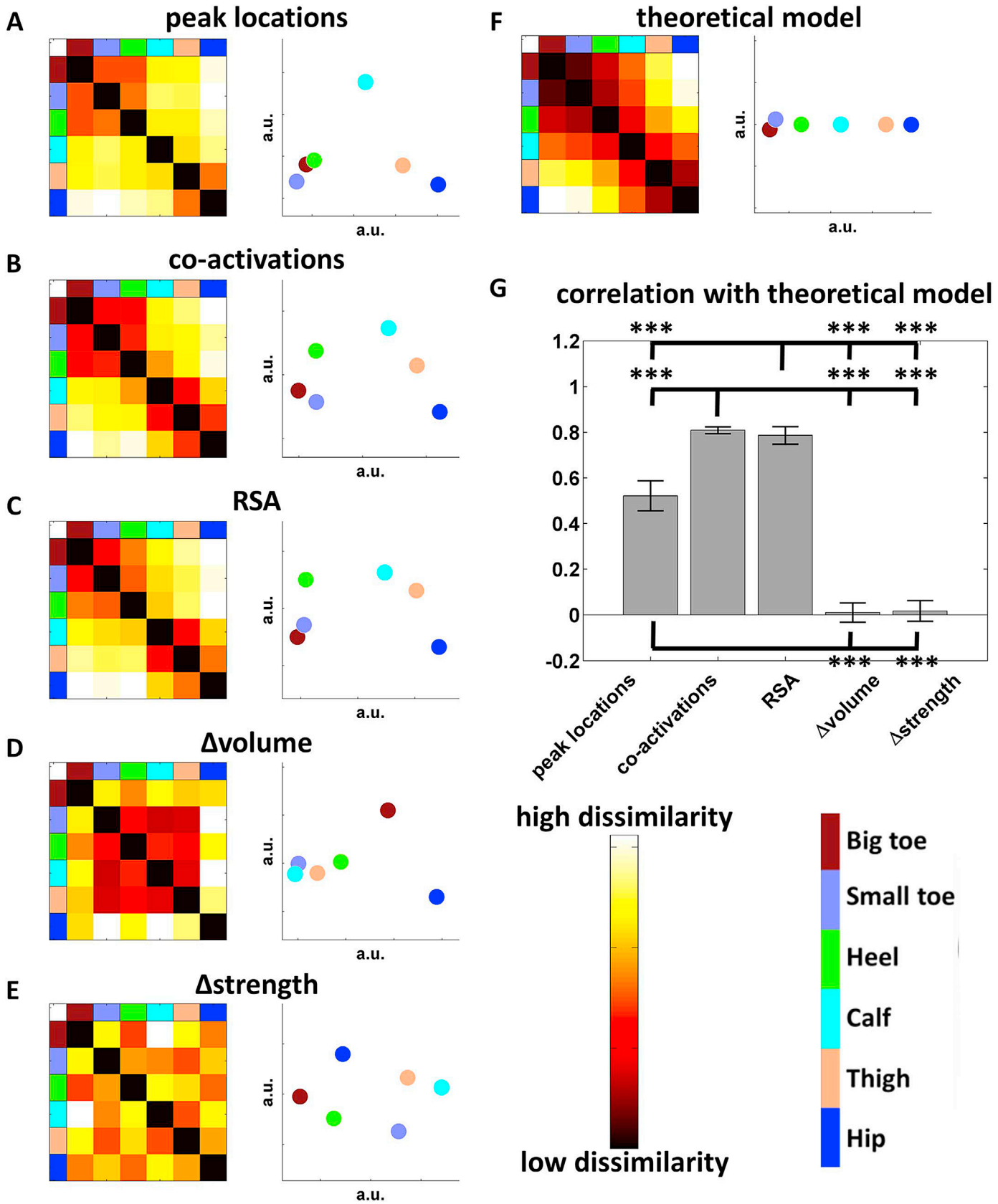


**Fig. 6.** Dissimilarity analysis. The dissimilarity matrices and corresponding 2D configurations based on classical multidimensional scaling are shown for the different measures. Data presented here are averaged across all BAs, data for separate BAs are presented in supplementary materials (Fig. S3–S8). a) "peak locations" dissimilarity based on the Euclidean distances between the cortical locations of pairs of S1 representations. b) "co-activations" dissimilarity based on the degree of reciprocal co-activation between pairs of S1 representations (see ISM.2 for details). c) "RSA" dissimilarity based on the cross-validated mahalanobis distance between the multi-voxel activity patterns in S1. d) "Δ volume" dissimilarity based on the differential volume of activation between pairs of S1 representations. e) "Δ strength" dissimilarity based on the differential strength of activation between pairs of S1 representations. f) Theoretical model of dissimilarity between pairs of body parts based on the physical structure of lower limbs (see ISM.3). g) Correlations between the 5 measures of dissimilarity and the theoretical model of lower limb structure. Significant post-hoc comparisons between the different measures of dissimilarity are shown with asterisks (* $p<0.05$, ** $p<0.01$, *** $p<0.001$).

section below on limitations of the study). In the present study, we rather focused on investigating the leg and foot, preventing us from more clearly determining a potential rostro-caudal somatotopic toe sequence for BAs in S1. Finally, concerning the location of the heel with respect to the toes, the sole representation in non-human primates lies adjacent to the toes along the rostro-caudal axis in BA 3b and along the caudo-rostral axis in BA 1 with a mirror reversal between the two (Merzenich et al., 1978; Kaas et al., 1979; Nelson et al., 1980). Future studies mapping the foot-leg region more completely will be required to determine if this is also found in humans.

Despite this evidence for somatotopy in the human S1 leg representation (that was weaker for the foot representations), we observed substantial inter-subject variability with respect to the exact sequence and location of each of the 12 mapped representations within S1. Such strong inter-individual variability was already reported for non-human primates (Merzenich et al., 1978), showing that a given body region is not at the same position in different individuals. This highlights the importance of studies focusing on single subject analysis to recover the detailed functional organization of primate S1. In particular, small cortical representations might not overlap at all across individuals, suggesting that generalizations based on group analysis should be regarded with caution. This may also explain the rather low number of publications describing lower limb somatotopy in S1 (using group-level analysis and lower spatial resolution) (Bao et al., 2012; Nakagoshi et al., 2005). We argue that this issue is less relevant for the hand, where the respective representations are larger and thus more likely to overlap across subjects, compatible with previously described somatotopic S1 organization of the upper limb at the group level (Gelnar et al., 1998; Kurth et al., 1998, 2000; Maldjian et al., 1999; van Westen et al., 2004). Studies targeting plasticity-dependent changes in S1 (Muret et al., 2016; Pleger et al., 2001), clinical research in amputees or spinal cord injury related to potential S1 changes in chronic pain (Freund et al., 2013; Henderson et al., 2011), and studies on phantom limb pain (Flor et al., 1995; Makin et al., 2013) should most likely pursue an approach that is based on high resolution single subject analysis.

Dissimilarity analysis showed that the anatomical properties of S1 representations, as measured by the locations of peak activations, were associated with the dimensions of the lower limbs in all investigated BAs, showing that S1 properties were strongly related to the physical structure of the lower limbs. This was further supported by our finding that the functional properties of S1 representations (co-activations and RSA) were also associated with the dimensions of the lower limbs in all investigated BAs (Ejaz et al., 2015).

*Lower selectivity in foot representations*

We also observed that the stimulation of a given toe consistently elicited activity increases not only in the stimulated toe representation, but also in non-stimulated representations of the same foot (other toe and the heel) while not activating regions of the leg (calf, thigh and hip). This was found for all mapped foot regions and across all BAs, suggesting that information is broadly processed in S1 foot representations, while still preferentially processed in the specific map. We detected further evidence for differences in S1 between leg and foot representations. Indeed, we also found a functional clustering of the lower limb representations, which linked the patterns of co-activations with the cortical distance between representations and seemed to follow a sigmoidal shape. We speculate that these foot-leg differences reflect differences in the functional properties of the foot and leg. Thus, most tactile stimulations at the level of the foot will likely stimulate many toes, the sole, and the heel simultaneously (especially during upright stance and walking). This differs from tactile stimulation of the leg (of calf, thigh and hip) that are less strongly linked during upright stance and walking, reflected by the more specific activations compared to foot stimulation and the absent activations in the foot areas in the present study. This finding for the foot representations also differs from hand/finger representations (Martuzzi et al., 2014), lending support (for the case of the lower limbs) to accounts of plasticity in S1 representations, whereby single body part maps are formed and maintained by the continuous competition and interaction between inputs from different body regions during activities of daily living (Buonomano and Merzenich, 1998; Serino and Haggard, 2010).

*Dominant representation of digit 1 of the foot*

Concerning the different body part representations, stimulation of the big toe was associated with stronger and more extensive activations compared to other foot (and leg) representations, suggesting a possible homology with the representation of the thumb, whose larger S1 representation has already been demonstrated in a recent ultra-high resolution study (Martuzzi et al., 2014) using an approach similar to that of the present study. Human thumb magnification was also hinted at in the classical work of Penfield and Boldrey (1937). One possible explanation for the over-representation of the thumb in humans is its extensive solicitation compared to other digits, which could also account for the importance of the big toe representation in the present study due to its greater mobility and control (and hence its respective larger and more frequent somatosensory input); alternatively this increase may reflect its greater importance for stance, balance and locomotion (Chou et al., 2009; Hughes et al., 1990). We note, however, that there is no evidence for magnification in non-human primates for digit 1 of the upper or lower limb (Merzenich et al., 1978; Kaas et al., 1979; Nelson et al., 1980), although this aspect was not directly investigated in these studies.

Interestingly, we also found greater extent and strength of BOLD responses for the hip representation, which is compatible with findings reported from neurophysiological studies in primates (Taoka et al., 2000). A possible interpretation of this result is that the tactile stimulation of the hip may have more likely also activated adjacent body regions of the trunk (i.e. the present "over-representation" of the hip may stem from the lack of competing neighboring representations located more laterally on the postcentral gyrus because we did not stimulate higher portions of the trunk or the chest). In addition, the trunk and hip are known to have tactile receptive fields with different receptive field properties (compared to hands and feet) and are known to be functionally relevant for tactile stimuli generating whole-body percepts (i.e. Blanke et al., 2015; Taoka et al., 2016). Finally, methodological factors could account for this result, such as more difficult access to this region during tactile stimulation in the 7 T scanner, possibly leading to larger or more variably stimulated skin regions.

*Bilateral representations in S1*

Unilateral hip (and trunk) stimulation has been shown to activate bilateral S1 regions and adjacent parietal regions in non-human primates (Taoka et al., 1998, 2000). Here we also found that, from all the stimulated body regions, only hip stimulation was associated with ipsilateral and contralateral S1 activations, revealing the presence of large and bilateral tactile S1 hip representations. Concerning the other mapped body parts, we observed no positive activations in ipsilateral S1 in response to tactile stimulation (except for hip stimulation) in all BAs and for all stimulated body regions, comparable with previous studies reporting BOLD deactivation in ipsilateral S1 (using median nerve stimulation; Nihashi et al., 2005; using tactile stimulation of the fingers; Hlushchuk and Hari, 2006) or motor representations of the lower limb (Ruddy et al., 2016).

*Differences across Brodmann areas*

Regarding differences across BAs, the extent of BOLD responses was smaller (but not weaker) in BA 2 compared to BA 3b and BA 1, independently from the represented body region in the left and right hemisphere. This suggests that the volume of leg and foot representations in BA 2 is reduced compared to BA 3b and 1 and extends previous human S1

findings using manual tactile finger stimulation to the leg/foot region of human S1 (Martuzzi et al., 2014, 2015; van der Zwaag et al., 2015). Although such differences may be related to differences in tactile processing in different S1 regions (i.e. differences in receptive field properties, coding of different tactile features; Costanzo and Gardner, 1980; Gardner, 1988; Iwamura, 1998) recent work using 7 T fMRI of S1 finger representations in humans has shown that the size of representations within BA 2 is smaller in comparison to BA 3b and BA 1 (Martuzzi et al., 2014, 2015) and that the activity induced by tactile finger stimulation across the different BAs depends on the modality of stimulation (van der Zwaag et al., 2015), in particular in BA 2, where finger activations were smallest. More work is necessary relating extent and strength of S1 activations to tactile processing and potential differences across S1 subregions.

We note that we did not find any apparent differences across BAs with respect to somatotopic selectivity, which was expected based on the known reduced selectivity in BA 2, as shown for finger representations (Besle et al., 2014; Martuzzi et al., 2014; Stringer et al., 2014). It is possible that differences in selectivity are less present for lower limbs compared to fingers and/or that the present study could not detect such evidence as only two, instead of all five toes were mapped (for further discussion see section on limitations of the present study below). However, it is also possible that the respective roles of the different BAs in tactile processing are not the same for the different body parts, such as foot, leg or fingers. In addition, the separation of the postcentral gyrus into BAs 3b, 1 and 2 might be improved using a functionally driven separation of the different BAs (Sanchez-Panchuelo et al., 2012), as this could be more precise and appropriate. However, the design of the present study did not allow such approach. Further studies directly comparing such aspects between lower and upper limbs are necessary.

### *Hemispheric differences*

Our data revealed no differences between left and right S1 concerning the somatotopic selectivity of BOLD responses in our right-footed participants and only few differences with respect to the extent and strength of BOLD responses within somatosensory representations. However, even for the hand, there is little or no evidence supporting hemispheric differences between the S1 representations of the left and right hands in right-handed subjects. Accordingly, several neuroimaging studies reported no differences between right and left hand representations (Boakye et al., 2000; Park et al., 2007; White et al., 1997). In particular, studies investigating morphological differences between right and left sensory-motor hand areas, both at the cellular scale using cytoarchitectonic measurements (White et al., 1997) and at the macroscopic scale using computed tomography imaging (Park et al., 2007), found no evidence for any asymmetries. In addition, Boakye et al. (2000) explicitly examined this issue, but did not report any interhemispheric differences between the BOLD activations observed in S1 during right and left median nerve stimulation.

### *Limitations of the study*

The present study has several limitations. We used manual stimulation and can therefore not exclude that subtle differences in the applied tactile stimulations may have affected the present S1 data. However, this should have rather introduced noise in our data, instead of impacting them in the systematic ways we reported. In particular, we took great care to stimulate all body parts repeatedly on a skin area of about 3 $cm^2$. This was the case for all body regions, except the small toe, which was stimulated on its entire length. Although this small toes stimulation could have induced a systematic bias, such a bias would have been limited to the representation of the small toe only and should have rather induced an overestimation of the small toe representation which was not the case (i.e. its full extent was mapped, but only a portion of the big toe was mapped). Nevertheless, these results should be regarded with caution and await confirmation. Finally, we note that we cannot exclude that habituation occurred during the tactile stimulation (i.e. we used blocks of 20 s) and that this may have affected certain body parts differently, although our stimulation protocol and analysis minimized this effect by the fixed-order of stimulation and by the GLM analysis.

Although leg-to-foot medio-lateral somatotopy was very consistent, our data were not characterized by a consistent ordering of the toes and heel representations across participants in the different subregions of S1. Thus, although the locations of foot representations were somatotopically ordered with respect to the rest of the leg representations, this was not the case for the three foot representations if compared among them. We argue that a design including the stimulation of the five toes would be more appropriate to further investigate and potentially distinguish between a potential latero-medial or rostro-caudal arrangement of toes. In addition, the investigation of the S1 representation of the five toes could potentially be more sensitive to highlight changes in selectivity across BAs, as it was demonstrated for fingers.

Finally, our study is limited by classical fMRI caveats, such as artifacts caused by draining vessels (Polimeni et al., 2010) or movement artifacts and we note that the complex and variable shape of the postcentral gyrus may have impacted the present data as it can lead to non-linear arrangements of body representation, which can be difficult to investigate in volumetric space. A surface-based analysis approach could have partially addressed this issue, but suffers from other limitations such as the necessity of adequately co-registering and segmenting structural images, as well as the difficulty to preserve small ROIs.

Future tactile mapping studies should consider classical mapping designs including stimulation of the entire body, continuous stimulation designs, and surface-based analyses (Huang et al., 2012; Sereno and Huang, 2014; Saadon-Grosman et al., 2015).

## Conclusions

The present study reports the mapping of the representation of lower limbs in different subregions of S1 (BAs 3b, 1 and 2) at the individual subject level, based on high-resolution fMRI. These data are important because, as compared to other sensory modalities (vision, audition), less is known about the organization of the human somatosensory system. By analyzing the localization, the somatotopic selectivity, the strength and extent of the different representations, we describe here the anatomical and functional properties of different lower limb representations. In particular, we showed that different sectors of the lower limb, namely the foot and the leg, have a different degree of selectivity in response to tactile stimulation and that certain body regions (i.e. big toe and hip) of the lower limbs have stronger and larger cortical representations in S1. These results were discussed in the context of a possible link between the functional properties of S1 representations and the degree of sensory stimulation received by the different regions of the lower limbs due to their specific functions. Importantly, we also showed that the anatomical and functional properties of S1 representations reflect the physical structure of lower limbs.

These data might have important implications for clinical and translational research in order to study plasticity in lower limb representations following different experimental manipulations (i.e. Muret et al., 2016; Pleger et al., 2001) as well as certain pathologies affecting the lower limb, such as amputation, vascular disease, diabetes, and spinal cord injury, in which the lower limbs are much more frequently affected than the upper limbs (Flor et al., 1995; Freund et al., 2013; Henderson et al., 2011; Makin et al., 2013).

## Acknowledgements

This work was supported by the Bertarelli Foundation and the National Competence Centre for Biomedical Imaging (NCCBI, Switzerland, grant number 591108).

## Appendix A. Supporting information

Supplementary data associated with this article can be found in the online version at doi:10.1016/j.neuroimage.2017.06.021.

## References


Bao, R., Wei, P., Li, K., Lu, J., Zhao, C., Wang, Y., Zhang, T., 2012. Within-limb somatotopic organization in human SI and parietal operculum for the leg: an fMRI study. Brain Res. 1445, 30–39. https://doi.org/10.1016/j.brainres.2012.01.029.

Besle, J., Sanchez-Panchuelo, R.-M., Bowtell, R., Francis, S., Schluppeck, D., 2014. Event-related fMRI at 7T reveals overlapping cortical representations for adjacent fingertips in S1 of individual subjects. Hum. Brain Mapp. 2043, 2027–2043. https://doi.org/10.1002/hbm.22310.

Blanke, O., Slater, M., Serino, A., 2015. Behavioral, Neural, and Computational Principles of Bodily Self-Consciousness. Neuron. https://doi.org/10.1016/j.neuron.2015.09.029.

Boakye, M., Huckins, S.C., Szeverenyi, N.M., Taskey, B.I., Hodge, C.J., 2000. Functional magnetic resonance imaging of somatosensory cortex activity produced by electrical stimulation of the median nerve or tactile stimulation of the index finger. J. Neurosurg. 93, 774–783. https://doi.org/10.3171/jns.2000.93.5.0774.

Buonomano, D.V., Merzenich, M.M., 1998. Cortical plasticity: from synapses to maps. Annu. Rev. Neurosci. 21, 149–186. https://doi.org/10.1146/annurev.neuro.21.1.149.

Chou, S.W., Cheng, H.Y.K., Chen, J.H., Ju, Y.Y., Lin, Y.C., Wong, M.K.A., 2009. The role of the great toe in balance performance. J. Orthop. Res. 27, 549–554. https://doi.org/10.1002/jor.20661.

Cnaan, A., Laird, N.M., Slasor, P., 1997. Using the general linear mixed model to analyse unbalanced repeated measures and longitudinal data. Stat. Med. 16, 2349–2380. https://doi.org/10.1002/(SICI)1097-0258(19971030)16:20.

Contini, R., 1972. Body segment parameters. Part II. Artif. Limbs 16, 1–19.

Costanzo, R.M., Gardner, E.P., 1980. A quantitative analysis of responses of direction-sensitive neurons in somatosensory cortex of awake monkeys. J. Neurophysiol. 43, 1319–1341.

Da Costa, S., van der Zwaag, W., Marques, J.P., Frackowiak, R.S.J., Clarke, S., Saenz, M., 2011. Human primary auditory cortex follows the shape of Heschl's gyrus. J. Neurosci.: Off. J. Soc. Neurosci. 31, 14067–14075. https://doi.org/10.1523/JNEUROSCI.2000-11.2011.

van der Zwaag, W., Francis, S., Head, K., Peters, A., Gowland, P., Morris, P., Bowtell, R., 2009. fMRI at 1. 5, 3 and 7 T: Characterising BOLD signal changes. NeuroImage 47, 1425–1434. https://doi.org/10.1016/j.neuroimage.2009.05.015.

van der Zwaag, W., Gruetter, R., Martuzzi, R., 2015. Stroking or Buzzing? A Comparison of somatosensory touch stimuli using 7 T fMRI. PLoS One 10, e0134610. https://doi.org/10.1371/journal.pone.0134610.

Ejaz, N., Hamada, M., Diedrichsen, J., 2015. Hand use predicts the structure of representations in sensorimotor cortex. Nat. Neurosci. 103, 1–10. https://doi.org/10.1038/nn.4038.

Flor, H., Elbert, T., Knecht, S., Wienbruch, C., 1995. Phantom-limb pain as a perceptual correlate of cortical reorganization following arm amputation. Science 375, 482–484.

Freund, P., Weiskopf, N., Ashburner, J., Wolf, K., Sutter, R., Altmann, D.R., Friston, K., Thompson, A., Curt, A., 2013. MRI investigation of the sensorimotor cortex and the corticospinal tract after acute spinal cord injury: a prospective longitudinal study. Lancet Neurol. 12, 873–881. https://doi.org/10.1016/S1474-4422(13)70146-7.

Gardner, E.P., 1988. Somatosensory cortical mechanisms of feature detection in tactile and kinesthetic discrimination. Can. J. Physiol. Pharmacol. 66, 439–454. https://doi.org/10.1139/y88-074.

Geisser, S., Greenhouse, S.W., 1958. An extension of box's results on the use of the F distribution in multivariate analysis. Ann. Math. Stat. 29, 885–891. https://doi.org/10.2307/2237272.

Gelnar, P.A., Krauss, B.R., Szeverenyi, N.M., Apkarian, A.V., 1998. Fingertip representation in the human somatosensory cortex: an fMRI study. NeuroImage 7, 261–283. https://doi.org/10.1006/nimg.1998.0341.

Geyer, S., Schleicher, A., Zilles, K., 1999. Areas 3a, 3b, and 1 of human primary somatosensory cortex. NeuroImage 10, 63–83. https://doi.org/10.1006/nimg.1999.0440.

Geyer, S., Schormann, T., Mohlberg, H., Zilles, K., 2000. Areas 3a, 3b, and 1 of human primary somatosensory cortex. Part 2. Spat. Norm. Stand. Anat. Space NeuroImage 11, 684–696. https://doi.org/10.1006/nimg.2000.0548.

Govindarajulu, Z., 1976. A brief survey of nonparametric statistics. Commun. Stat. - Theory Methods 5 (5), 429–453. https://doi.org/10.1080/03610927608827365.

Grefkes, C., Geyer, S., Schormann, T., Roland, P., Zilles, K., 2001. Human somatosensory area 2: observer-independent cytoarchitectonic mapping, interindividual variability, and population map. NeuroImage 14, 617–631. https://doi.org/10.1006/nimg.2001.0858.

Henderson, L.A.a., Gustin, S.M., Macey, P.M., Wrigley, P.J., Siddall, P.J., 2011. Functional reorganization of the brain in humans following spinal cord injury: evidence for underlying changes in cortical anatomy. J. Neurosci.: Off. J. Soc. Neurosci. 31, 2630–2637. https://doi.org/10.1523/JNEUROSCI.2717-10.2011.

Hlushchuk, Y., Hari, R., 2006. Transient suppression of Ipsilateral primary somatosensory cortex during tactile finger stimulation. J. Neurosci. 26, 5819–5824. https://doi.org/10.1523/JNEUROSCI.5536-05.2006.

Huang, R.-S., Chen, C., Tran, A.T., Holstein, K.L., Sereno, M.I., 2012. Mapping multisensory parietal face and body areas in humans. Proc. Natl. Acad. Sci. USA 109, 18114–18119. https://doi.org/10.1073/pnas.1207946109.

Hughes, J., Clark, P., Klenerman, L., 1990. The importance of the toes in walking. J. Bone Jt. Surg. Br. 72, 245–251.

Iwamura, Y., 1998. Hierarchical somatosensory processing. Curr. Opin. Neurobiol. 8, 522–528.

Jones, E.G., Coulter, J.D., Hendry, S.H., 1978. Intracortical connectivity of architectonic fields in the somatic sensory, motor and parietal cortex of monkeys. J. Comp. Neurol. 181, 291–347. https://doi.org/10.1002/cne.901810206.

Kaas, J., Nelson, R., Sur, M., Lin, C., Merzenich, M., 1979. Multiple representations of the body within the primary somatosensory cortex of primates. Science 204, 1977–1979.

Kriegeskorte, N., Mur, M., Bandettini, P., 2008. Representational similarity analysis - connecting the branches of systems neuroscience. Front. Syst. Neurosci. 2, 4. https://doi.org/10.3389/neuro.06.004.2008.

Kurth, R., Villringer, K., Mackert, B.M., Schwiemann, J., Braun, J., Curio, G., Villringer, a., Wolf, K.J., 1998. FMRI assessment of somatotopy in human Brodmann area 3b by electrical finger stimulation. Neuroreport 9, 207–212.

Kurth, R., Villringer, K., Curio, G., Wolf, K.J., Krause, T., Repenthin, J., Schwiemann, J., Deuchert, M., Villringer, A., 2000. FMRI shows multiple somatotopic digit representations in human primary somatosensory cortex. Neuroreport 11, 1–5. https://doi.org/10.1097/00001756-200005150-00025.

Makin, T.R., Scholz, J., Filippini, N., Slater, D.H., Tracey, I., Johansen-berg, H., Henderson Slater, D., 2013. Phantom pain is associated with preserved structure and function in the former hand area. Nat. Commun. 4, 1570. https://doi.org/10.1038/ncomms2571.

Maldjian, J.A., Gottschalk, A., Patel, R.S., Detre, J.A., Alsop, D.C., 1999. The sensory somatotopic map of the human hand demonstrated at 4 T. NeuroImage 10, 55–62. https://doi.org/10.1006/nimg.1999.0448.

Marques, J.P., Kober, T., Kruegger, G., van der Zwaag, W., Van de Moortele, P.F., Gruetter, R., 2010. MP2RAGE, a self-bias field corrected sequence for improved segmentation at high field. NeuroImage 49, 1271–1281. https://doi.org/10.1016/j.neuroimage.2009.10.002.

Martuzzi, R., van der Zwaag, W., Farthouat, J., Gruetter, R., Blanke, O., 2014. Human finger somatotopy in areas 3b, 1, and 2: a 7T fMRI study using a natural stimulus. Hum. Brain Mapp. 35, 213–226. https://doi.org/10.1002/hbm.22172.

Martuzzi, R., van der Zwaag, W., Dieguez, S., Serino, A., Gruetter, R., Blanke, O., 2015. Distinct contributions of Brodmann areas 1 and 2 to body ownership. Soc. Cogn. Affect. Neurosci. 1–11. https://doi.org/10.1093/scan/nsv031.

Merzenich, M.M., Kaas, J.H., Sur, M., Lin, C.S., 1978. Double representation of the body surface within cytoarchitectonic areas 3b and 1 in "SI" in the owl monkey (Aotus trivirgatus). J. Comp. Neurol. 181, 41–73. https://doi.org/10.1002/cne.901810104.

Muret, D., Daligault, S., Dinse, H.R., Delpuech, C., Mattout, J., Reilly, K.T., Farnè, A., Farne, A., 2016. Neuromagnetic correlates of adaptive plasticity across the hand-face border in human primary somatosensory cortex. J. Neurophysiol. 2095–2104. https://doi.org/10.1152/jn.00628.2015.

Nakagoshi, A., Fukunaga, M., Umeda, M., Mori, Y., Higuchi, T., Tanaka, C., 2005. Somatotopic representation of acupoints in human primary somatosensory cortex: an FMRI study. Magn. Reson. Med. Sci.: Offc. J. Jpn. Soc. Magn. Reson. Med. 4, 187–189.

Nelson, R.J., Sur, M., Felleman, D.J., Kaas, J.H., 1980. Representations of the body surface in postcentral parietal cortex of Macaca fascicularis. J. Comp. Neurol. 192, 611–643. https://doi.org/10.1002/cne.901920402.

Nihashi, T., Naganawa, S., Sato, C., Kawai, H., Nakamura, T., Fukatsu, H., Ishigaki, T., Aoki, I., 2005. Contralateral and ipsilateral responses in primary somatosensory cortex following electrical median nerve stimulation–an fMRI study. Clin. Neurophysiol.: Offc. J. Int. Fed. Clin. Neurophysiol. 116, 842–848. https://doi.org/10.1016/j.clinph.2004.10.011.

Nili, H., Wingfield, C., Walther, A., Su, L., Marslen-Wilson, W., Kriegeskorte, N., 2014. A toolbox for Representational similarity analysis. PLoS Comput. Biol. 10, e1003553. https://doi.org/10.1371/journal.pcbi.1003553.

Oldfield, R.C., 1971. The assessment and analysis of handedness: the Edinburgh inventory. Neuropsychologia 9, 97–113. https://doi.org/10.1016/0028-3932(71)90067-4.

Olman, C.A., Van de Moortele, P.F., Schumacher, J.F., Guy, J.R., Uğurbil, K., Yacoub, E., 2010. Retinotopic mapping with spin echo BOLD at 7T. Magn. Reson. Imaging 28, 1258–1269. https://doi.org/10.1016/j.mri.2010.06.001.

Overduin, S.A., Servos, P., 2004. Distributed digit somatotopy in primary somatosensory cortex. NeuroImage 23, 462–472. https://doi.org/10.1016/j.neuroimage.2004.06.024.

Page, E., 1963. Ordered hypotheses for multiple treatments: a significance test for linear ranks. J. Am. Stat. Assoc. 58, 216–230. https://doi.org/10.1080/01621459.1963.10500843.

Park, M.C., Goldman, M.A., Park, M.J., Friehs, G.M., 2007. Neuroanatomical localization of the "precentral knob" with computed tomography imaging. Stereotact. Funct. Neurosurg. 85, 158–161. https://doi.org/10.1159/000099074.

Penfield, W., Boldrey, E., 1937. Somatic motor and sensory representation in the cerebral cortex of man as studied by electrical stimulation. Brain.

Pfannmöller, J.P., Greiner, M., Balasubramanian, M., Lotze, M., 2016. High-resolution fMRI investigations of the fingertip somatotopy and variability in BA3b and BA1 of the primary somatosensory cortex. Neuroscience 339, 667–677.

Pleger, B., Dinse, H.R., Ragert, P., Schwenkreis, P., Malin, J.P., Tegenthoff, M., 2001. Shifts in cortical representations predict human discrimination improvement. Proc. Natl. Acad. Sci. USA 98, 12255–12260. https://doi.org/10.1073/pnas.191176298.

Polimeni, J.R., Fischl, B., Greve, D.N., Wald, L.L., 2010. Laminar analysis of 7 T BOLD using an imposed spatial activation pattern in human V1. NeuroImage 52, 1334–1346.

Rasmussen, T., Penfield, W., 1947. Further studies of the sensory and motor cerebral cortex of man. Fed. Proc. 6, 452–460.

Ruddy, K.L., Jaspers, E., Keller, M., Wenderoth, N., 2016. Interhemispheric sensorimotor integration; an upper limb phenomenon? Neuroscience 333, 104–113. https://doi.org/10.1016/j.neuroscience.2016.07.014.

Saadon-Grosman, N., Tal, Z., Itshayek, E., Amedi, A., Arzy, S., 2015. Discontinuity of cortical gradients reflects sensory impairment. Proc. Natl. Acad. Sci. USA 112, 16024–16029. https://doi.org/10.1073/pnas.1506214112.

Salomon, R., Darulova, J., Narsude, M., van der Zwaag, W., 2014. Comparison of an 8-channel and a 32-channel coil for high-resolution FMRI at 7 T. Brain Topogr. 27, 209–212. https://doi.org/10.1007/s10548-013-0298-6.

Sanchez-Panchuelo, R.M., Francis, S., Bowtell, R., Schluppeck, D., 2010. Mapping human somatosensory cortex in individual subjects with 7T functional MRI. J. Neurophysiol. 2544–2556. https://doi.org/10.1152/jn.01017.2009.

Sanchez-Panchuelo, R.M., Besle, J., Beckett, A., Bowtell, R., Schluppeck, D., Francis, S., 2012. Within-digit functional parcellation of Brodmann areas of the human primary somatosensory cortex using functional magnetic resonance imaging at 7 T. J. Neurosci. 32, 15815–15822. https://doi.org/10.1523/JNEUROSCI.2501-12.2012.

Schweizer, R., Voit, D., Frahm, J., 2008. Finger representations in human primary somatosensory cortex as revealed by high-resolution functional MRI of tactile stimulation. NeuroImage 42, 28–35. https://doi.org/10.1016/j.neuroimage.2008.04.184.

Seber, G.A.F., 1984. Multivariate Observations. John Wiley&Sons, Inc., Hoboken, NJ.

Sereno, M.I., Huang, R.S., 2014. Multisensory maps in parietal cortex. Curr. Opin. Neurobiol. https://doi.org/10.1016/j.conb.2013.08.014.

Serino, A., Haggard, P., 2010. Touch and the body. Neurosci. Biobehav. Rev. https://doi.org/10.1016/j.neubiorev.2009.04.004.

Speck, O., Stadler, J., Zaitsev, M., 2008. High resolution single-shot EPI at 7T. Magn. Reson. Mater. Phys., Biol. Med. 21, 73–86. https://doi.org/10.1007/s10334-007-0087-x.

Stringer, E., Qiao, P.-G., Friedman, R.M., Holroyd, L., Newton, A.T., Gore, J.C., Min Chen, L., 2014. Distinct fine-scale fMRI activation patterns of contra- and ipsilateral somatosensory areas 3b and 1 in humans. Hum. Brain Mapp. 35, 4841–4857. https://doi.org/10.1002/hbm.22517.

Stringer, E.A., Chen, L.M., Friedman, R.M., Gatenby, C., Gore, J.C., 2011. Differentiation of somatosensory cortices by high-resolution fMRI at 7 T. NeuroImage 54, 1012–1020. https://doi.org/10.1016/j.neuroimage.2010.09.058.

Taoka, M., Toda, T., Iwamura, Y., 1998. Representation of the midline trunk, bilateral arms, and shoulders in the monkey postcentral somatosensory cortex. Exp. Brain Res. Exp. Hirnforsch. Exp. Céréb. 123, 315–322. https://doi.org/10.1007/s002210050574.

Taoka, M., Toda, T., Iriki, A., Tanaka, M., Iwamura, Y., 2000. Bilateral receptive field neurons in the hindlimb region of the postcentral somatosensory cortex in awake macaque monkeys. Exp. Brain Res. 134, 139–146. https://doi.org/10.1007/s002210000464.

Taoka, M., Toda, T., Hihara, S., Tanaka, M., Iriki, A., Iwamura, Y., 2016. A systematic analysis of neurons with large somatosensory receptive fields covering multiple body regions in the secondary somatosensory area of macaque monkeys. J. Neurophysiol. 116, 2152–2162. https://doi.org/10.1152/jn.00241.2016.

Weibull, A., Björkman, A., Hall, H., Rosén, B., Lundborg, G., Svensson, J., 2008. Optimizing the mapping of finger areas in primary somatosensory cortex using functional MRI. Magn. Reson. Imaging 26, 1342–1351. https://doi.org/10.1016/j.mri.2008.04.007.

van Westen, D., Fransson, P., Olsrud, J., Rosén, B., Lundborg, G., Larsson, E.-M., Van Westen, D., 2004. Finger somatotopy in area 3b: an fMRI-study. BMC Neurosci. 5, 28. https://doi.org/10.1186/1471-2202-5-28.

White, L.E., Andrews, T.J., Hulette, C., Richards, A., Groelle, M., Paydarfar, J., Purves, D., 1997. Structure of the human sensorimotor system. II: lateral symmetry. Cereb. Cortex 7, 31–47. https://doi.org/10.1093/cercor/7.1.31.

Wilcoxon, F., 1946. Individual comparisons of grouped data by ranking methods. J. Econ. Entomol. 39, 269. https://doi.org/10.2307/3001968.

Zeharia, N., Hertz, U., Flash, T., Amedi, A., 2015. New whole-body sensory-motor gradients revealed using phase-locked analysis and verified using multivoxel pattern analysis and functional connectivity. J. Neurosci.: Off. J. Soc. Neurosci. 35, 2845–2859. https://doi.org/10.1523/JNEUROSCI.4246-14.2015.